Volume 12
Number 11
21 March 2021
Pages 3791–4186

Chemical Science

rsc.li/chemical-science

ISSN 2041-6539

ROYAL SOCIETY OF CHEMISTRY

EDGE ARTICLE
Masaki Horie *et al.*
Ring rotation of ferrocene in interlocked molecules in single crystals

Chemical Science

ROYAL SOCIETY OF CHEMISTRY

EDGE ARTICLE

View Article Online
View Journal | View Issue

Cite this: *Chem. Sci.*, 2021, **12**, 3871

All publication charges for this article have been paid for by the Royal Society of Chemistry

Received 17th December 2020
Accepted 21st January 2021

DOI: 10.1039/d0sc06876d

rsc.li/chemical-science

Ring rotation of ferrocene in interlocked molecules in single crystals†

Chi-Hsien Wang,[a] Kai-Jen Chen,[a] Tsung-Huan Wu,[a] Hung-Kai Chang,[a] Yoshitaka Tsuchido,[bc] Yoshihisa Sei,[d] Pei-Lin Chen[e] and Masaki Horie *[a]

This work describes unique molecular motions of ferrocene-containing interlocked molecules observed by single-crystal X-ray crystallography. The rotational flexibility of ferrocene is achieved using combinations of ferrocene-tethered ammonium and 30-membered ring dibenzo-crown ether. By contrast, ferrocene was locked in the complex with an 18-membered ring dibenzo-crown ether and CH_2Cl_2. When the complex was heated at 358 K, CH_2Cl_2 was removed from the complex, which led to drastic structural changes, including a semieclipsed-to-disordered transition of ferrocene and flipping of the dibenzo-crown ether.

Introduction

Ferrocene is one of the most attractive organometallic complexes because of its unique sandwich structure and characteristics.[1–4] Since its discovery, ferrocene and its derivatives have been extensively investigated in both fundamental and application studies. For instance, certain ferrocene derivatives were found to function as efficient redox catalysts, remotely controlling the reactivity of metal complexes and tailoring the activity of ring-opening polymerization.[5,6] Other examples include multi-ferrocenyl complexes with controlled mixed valence states,[7,8] and cyclic ferrocene derivatives that have been used as monomers for ring-opening polymerization, leading to self-assembled supramolecular architectures.[9] Furthermore, ferrocene has been encapsulated in metal–organic frameworks, showing electrochemical activity[10] and motion flexibility.[11]

The internal rotation of the cyclopentadienyl (Cp) rings along the Cp–Fe–Cp axis gives the eclipsed or staggered conformer with D_{5h} or D_{5d} point symmetry, respectively (Fig. 1A).[4,12] However, ferrocene has been reported to adopt the staggered form in the crystalline state because of the presence of multiple intermolecular CH–π interactions between its Cp

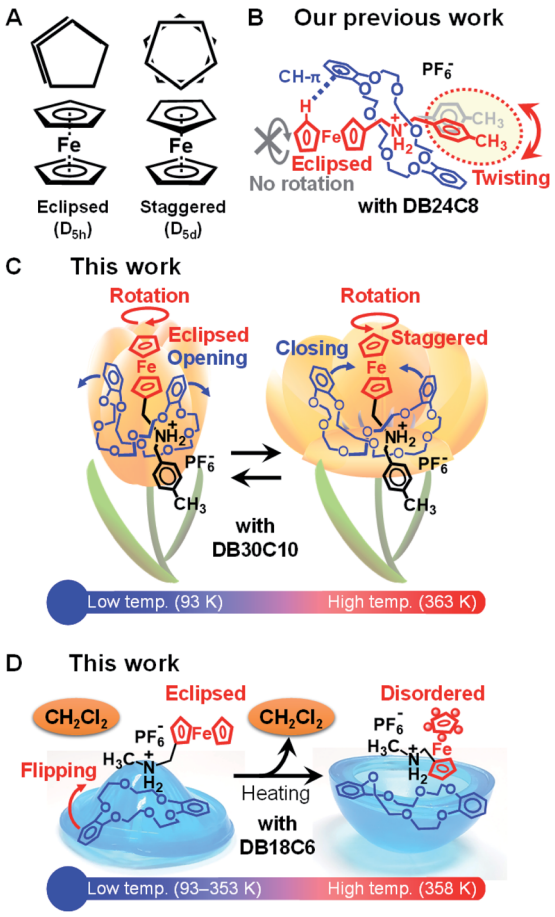

Fig. 1 (A) Eclipsed and staggered forms of ferrocene. (B) Twisting of the tolyl group accompanied by a crystal-to-crystal phase transition of DB24C8-containing pseudorotaxane. (C) Internal rotation of ferrocene in DB30C10-containing pseudorotaxane. (D) Flipping of DB18C6 and disordering of ferrocene in the DB18C6-containing complex.

[a]*Department of Chemical Engineering, National Tsing Hua University, 101, Section 2, Kuang-Fu Road, Hsinchu 30013, Taiwan. E-mail: mhorie@mx.nthu.edu.tw*

[b]*Laboratory for Chemistry and Life Science, Institute of Innovative Research, Tokyo Institute of Technology, 4259 Nagatsuta, Midori-ku, Yokohama 226-8503, Japan*

[c]*Department of Chemistry, Faculty of Science, Tokyo University of Science, 1-3 Kagurazaka, Shinjuku-ku, Tokyo 162-8601, Japan*

[d]*Open Facility Center, Tokyo Institute of Technology, 4259 Nagatsuta, Midori-ku, Yokohama 226-8503, Japan*

[e]*Instrumentation Center, National Tsing Hua University, 101, Section 2, Kuang-Fu Road, Hsinchu 30013, Taiwan*

† Electronic supplementary information (ESI) available: Experimental details, material characterization data and crystallographic details. CCDC 2033783–2033808. For ESI and crystallographic data in CIF or other electronic format see DOI: 10.1039/d0sc06876d

rings.[13] Nevertheless, some authors have demonstrated the rotational flexibility of ferrocene in the crystalline state.[14,15] For example, an irreversible eclipsed–disordered transition of ferrocene was observed in a hexafluorobenzene solvate crystal.[15] Motions of ferrocene have been theoretically calculated and observed by spectroscopic techniques such as infrared and ^{1}H and solid state ^{13}C NMR spectroscopies.[4,11,12,16–18] Because ferrocene has a very low rotation barrier of only 4 kJ mol^{-1},[4,16,17] it has been used as a building block for rotary molecular switches, where the rotational motion of ferrocene is induced by pressure, light, pH, solvent, or substituents.[3,19,20] However, the internal rotation—in particular, the reversible eclipsed–staggered conversion of ferrocene—has not been directly observed by single-crystal X-ray crystallography.

Molecular machines and switches have attracted great interest because they can transduce external stimuli such as chemical, photochemical, and electrochemical reactions into mechanical motions at the molecular level.[21–26] Among them, interlocked molecules, such as rotaxanes and pseudorotaxanes consisting of an axle component threading into a cyclic component exhibited relative position changes in response to external stimuli.[21–26] We have reported thermally and photoinduced deformation and bending of pseudorotaxane crystals.[26–30] The crystal-to-crystal phase transition illustrated in Fig. 1B was observed in a pseudorotaxane crystal comprising a ferrocene-tethered ammonium axle and dibenzo[24]crown-8 ether (DB24C8). The phase transition was accompanied by twisting of the tolyl group of the axle molecule upon heating at 401 K. In this transition, the pseudorotaxane structure played a critical role in providing molecular flexibility even in the crystal state. However, the eclipsed form of ferrocene was preserved by C–H···π interaction between the H atom of the Cp ring and one of the catechol rings of DB24C8 during the temperature change.

Because the motion of ferrocene is strongly influenced by the dibenzo-crown ether in the interlocked molecular systems, modifying their components by varying size of the dibenzo-crown ether and the length of the ferrocene-tethered ammonium moiety is important for imparting ferrocene with motion flexibility. Here, we report unique molecular motions of ferrocene-containing interlocked molecules in the crystal state. These motions were directly observed by single-crystal X-ray crystallography. Fig. 1C shows a schematic of the thermally induced rotation of ferrocene in a pseudorotaxane complex. This conversion was achieved using a large cyclic molecule of dibenzo[30]crown-10 ether (DB30C10) in which two catechol rings open, accompanied by the rotation of ferrocene, at high temperatures. Such motion resembles a flower blossoming: flower buds (*e.g.*, tulip) are well known to open and close at high and low temperatures, respectively. Similar ferrocenyl rotation was also observed in the interlocked molecule comprising a small cyclic molecule of dibenzo[18]crown-6 ether (DB18C6). In addition, its solvate complex with CH_2Cl_2 exhibited flipping of the DB18C6 upon removal of CH_2Cl_2 by heating, leading to the semieclipsed-to-disordered transition of ferrocene (Fig. 1D). Such flipping motion of the cyclic molecule from convexity to concavity resembles the motion of a rubber popper toy.

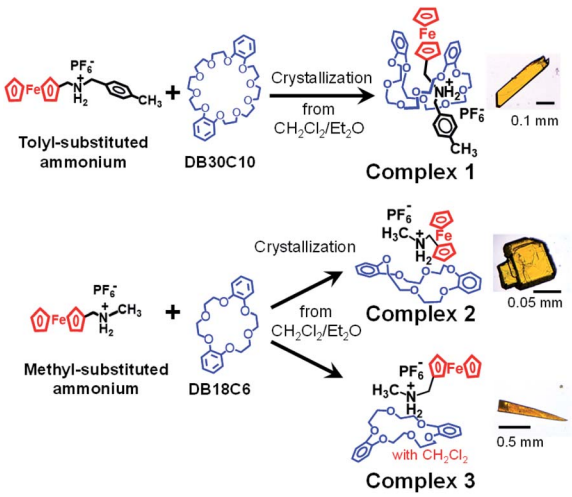

Scheme 1 Formation of single crystals of complexes **1**–**3**.

Results and discussion

Scheme 1 shows the preparation of crystals of interlocked complexes **1**–**3**. Their single crystals were obtained by mixing an ammonium salt and a dibenzo-crown ether in CH_2Cl_2, followed by diffusion of diethyl ether into the solution under ambient conditions. Complex **1** is composed of bulky tolyl-substituted ferrocenylmethyl ammonium and the large dibenzo-crown ether DB30C10, leading to the pseudorotaxane structure. By contrast, a combination of a short methyl-substituted ferrocenylmethyl ammonium with a small dibenzo-crown ether (DB18C6) provided two types of crystals that were separated as yellowish blocks (**2**) and thin plates (**3**). In later analysis, we observed that **3** contained CH_2Cl_2 solvent molecules, which played an important role in dynamic molecular motions in the crystal state. The characterization results are summarized in Fig. S1–S6.†

Fig. 2A shows the molecular structure of **1** obtained by single-crystal X-ray crystallography at 93 K. The interlocked structure of the pseudorotaxane was formed by N–H···O hydrogen bondings between the axle ammonium and DB30C10 at the center of the complex. In this complex, DB30C10 assumed a boat conformation in which two catechol groups were folded to surround ferrocene. By contrast, the combination of intermediate-sized DB24C8 and the same axle ammonium has been reported to result in the chair form of DB24C8 (Fig. 1B).[26,27] The internal rotation angle between the two Cp rings of ferrocene was estimated to be 11.0°, which is assigned to the semi-eclipsed form. According to our previous reports, ferrocene in most [2]pseudorotaxane crystals exhibits the eclipsed form with a much smaller rotation angle (<4°).[26–29] Based on this comparison, we speculated that the ferrocene in **1** would exhibit rotational flexibility.

Fig. 2B shows the molecular structure of **2** at 100 K. Because of the combination of the small cyclic molecule and the short ammonium, the N atom was surrounded by O atoms of DB18C6 *via* N–H···O hydrogen bondings, without the ammonium being

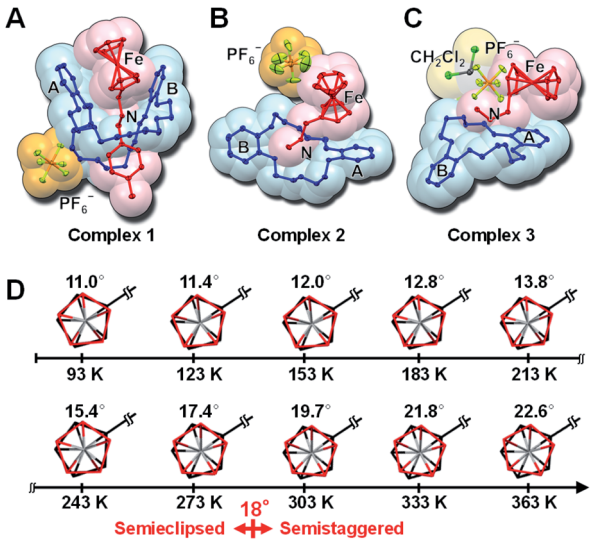

Fig. 2 Single-crystal X-ray crystallographic structures of (A) **1** at 93 K, (B) **2** at 100 K, and (C) **3** at 93 K (ellipsoid plot with 50% probability). (D) Top view of the ferrocenyl group of **1** at various temperatures.

threaded into the cyclic molecule. In this complex, DB18C6 adopted a twisted-chair form. The ferrocene stood on catechol ring A of DB18C6 with the face-on arrangement. This conformation was stabilized by π–π interaction between the ammonium-tethered Cp and catechol ring A. The other Cp ring without a substituent exhibited an elongated ellipsoid shape in the horizontal direction, implying rotational flexibility of the ferrocene.

Fig. 2C shows the molecular structure of **3** at 93 K. We found that **3** was a solvate complex between **2** and CH_2Cl_2 but that its conformation was quite different from that of **2**. In this complex, DB18C6 assumed a boat conformation. Ferrocene lies on catechol ring A in an edge-on arrangement. Because these components were tightly packed with CH_2Cl_2, the ellipsoid shape of both Cp rings was small; they were presumably locked.

To observe heat-induced structural changes of **1**–**3**, single-crystal X-ray crystallography was conducted at various temperatures. Detailed data are summarized in Fig. S7–S10 and Tables S1–S5.† We found interesting conformational changes in **1**: internal rotation of ferrocene and a slight opening of the folded catechol groups. These changes were reversible in the temperature range between 93 K and 363 K (Tables S1 and S2†). Fig. 2D shows the top view of ferrocene along Cp–Fe–Cp at various temperatures. Upon heating, ferrocene gradually rotated and finally reached 22.6°, which was assigned to the semistaggered form, at 363 K. Because the rotation of two pentagonal Cp rings is considered, the threshold rotation angle is defined as 18.0° for the eclipsed–staggered conversion. Thus, the observed threshold temperature was slightly greater than 273 K.

To discuss detailed structural changes, we plotted the temperature dependence of the internal rotation angle and the distance between Cp rings of the ferrocene in Fig. 3A and B, respectively. As the rotation angle increased, the Cp–Cp distance slightly decreased from 3.30 Å (at 93 K) to 3.28 Å (at 363 K) because the staggered form has less steric repulsion between H atoms of the two Cp rings. The temperature dependence of intramolecular interactions in **1** was also analyzed. The C–H···π distance, which is the distance between the C–H of unsubstituted Cp and a centroid of one of the catechol rings (ring A in Fig. 2A), is shown in Fig. 3C. Upon heating at temperatures less than 273 K, the C–H···π distance was maintained at ~3.27 Å. At temperatures greater than the threshold temperature of 273 K, the C–H···π distance increased substantially, finally reaching 3.37 Å at 363 K. In addition, the distance between the two catechol rings (A–B in Fig. 2A) gradually increased when the complex was heated, meaning that the folded DB30C10 opened slightly (Fig. 3D).

Similar to **1**, ferrocene in **2** adopted the semieclipsed form at 100 K, with an internal rotation angle of 10.9°, which gradually increased to 17.2° at 340 K (Fig. 3E). However, the crystal melted at temperatures greater than 340 K before the ferrocene achieved the staggered conformation. Upon heating, the plane angle between the two catechol rings (A–B in Fig. 2B) gradually increased from 102.6° (at 100 K) to 104.4° (at 340 K), suggesting that the twisted-chair structure of DB18C6 opened slightly (Fig. 3F).

By contrast, the internal rotation angle of the ferrocene in **3** varied by less than 1° (8.0° at 93 K and 8.7° at 358 K) (Fig. 3G). In

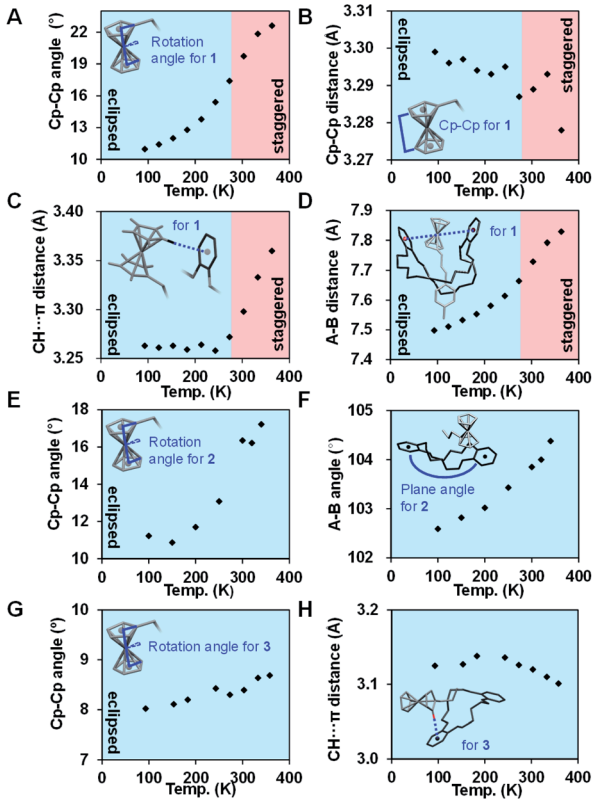

Fig. 3 Temperature dependence of the (A) Cp–Cp rotation angle for **1**, (B) Cp–Cp distance for **1**, (C) C–H···π distance for **1**, (D) catechol A–B distance for **1**, (E) Cp–Cp rotation angle for **2**, (F) catechol A–B plane angle for **2**, (G) Cp–Cp rotation angle for **3**, and (H) C–H···π distance for **3**.

addition, the C–H···π distance between ammonium-tethered Cp and catechol ring A remained slightly longer than 3.1 Å at temperatures less than 358 K (Fig. 3H). Nevertheless, we observed interesting thermodynamic features of **3** upon heating it to temperatures greater than 358 K.

Fig. 4A shows optical micrographs of a crystal of **3** under cross-polarized light. Interference color was observable at 303 K, whereas the color was gradually degraded at 358 K, suggesting the occurrence of the crystal-to-crystal phase transition. This color change was irreversible upon cooling to 303 K. Further heating to temperatures greater than 423 K immediately melted the crystal. To investigate the thermal properties of crystals of **3**, we carried out differential scanning calorimetry (DSC; Fig. 4B). During the heating scan, an endothermic peak was observed at 358 K, consistent with the interference color change. The thermodynamic parameters were estimated to be $\Delta H = 28$ kJ mol^{-1} and $\Delta S = 78$ J mol^{-1} K^{-1}, accompanied by the phase transition.

After crystals of **3** were heated at 358 K for 2 min, they were analyzed by single-crystal X-ray crystallography (Fig. 4C and D and Tables S4 and S5†). We found that CH_2Cl_2 was absent from the resulting structure and that this structure was very similar to that of **2**. Specific structural changes are summarized as follows: (i) the unsubstituted Cp ring and PF_6^- were disordered, (ii) ferrocene was flipped from horizontal to vertical with respect to catechol ring A, (iii) DB18C6 was flipped from the boat form to the twisted-chair form, (iv) the ammonium chain was transformed from a concave shape to a zigzag shape.

We now consider the effect of the molecular structures of the interlocked complexes on the mechanical molecular motions in single crystals. Because the motions of the molecular components are partially restricted in the highly ordered molecular packing within the crystal, the internal rotational motion was preferentially observed in interlocked complexes **1** and **2** because of the flexible feature of dibenzo-crown ethers. The ferrocene in **1** was surrounded by two catechol rings of folded DB30C10. Within DB30C10, the internal rotation of ferrocene was strongly correlated with intramolecular interactions in the pseudorotaxane structure. In particular, the C–H···π interaction between ferrocene and DB30C10 provided the critical effect, controlling the rotation flexibility of ferrocene. The unsubstituted Cp ring was released from the restriction of C–H···π interaction, accompanied by opening of the two catechol rings at temperatures greater than 273 K. The internal rotation of ferrocene in **2** was controlled by different factors. Ferrocene in **2** stood on an ammonium-tethered catechol ring, forming π–π interactions. Because DB18C6 adopted the metastable twisted-chair formation, the opening motion of the two catechol rings was induced at high temperatures, disrupting the π–π interaction. This opening motion of DB18C6 weakened the π–π interaction, inducing the internal rotation of ferrocene.

By contrast, the internal rotation of ferrocene was locked in **3** because of the C–H···π interaction between Cp and catechol A as well as the tightly packed crystal structure with CH_2Cl_2 at temperatures less than 358 K. Nevertheless, the locking effect was released by the removal of CH_2Cl_2 at temperatures greater than 358 K, affording rotatable ferrocene. During the crystal-to-crystal phase transition, drastic structural changes (*i.e.*, flipping of ferrocene and DB18C6) were achieved because of the flexible features of the interlocked complex without threading. The observed thermodynamic parameters were approximately four times greater than those for the flipping of a tolyl group accompanied by the crystal-to-crystal phase transition of pseudorotaxane comprising tolyl-substituted ammonium with DB24C8 (Fig. 1B).[27]

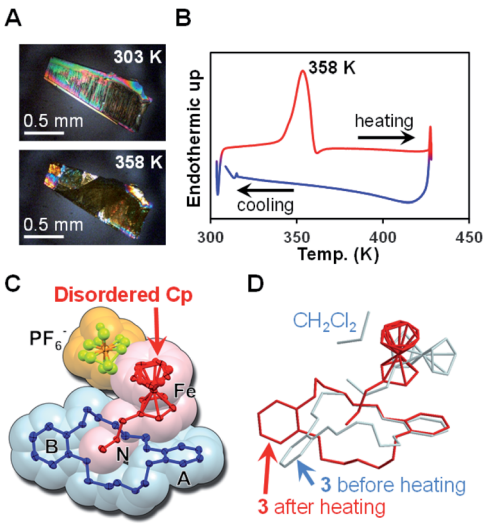

Fig. 4 (A) Optical micrographs of a single crystal of **3** at 303 K and 358 K under cross-polarized light. (B) DSC heating and cooling scans for crystals of **3** at a scan rate of 5 K min^{-1}. (C) Single-crystal X-ray crystallographic structure of **3** at 100 K after the sample was heated at 358 K for 2 min (ellipsoid plot with 50% probability). (D) Overlay of the molecular structures of **3** before and after heating at 358 K (light-blue and red, respectively). The counter anion was omitted for clarity. See also the ESI Movie.†

Conclusion

To the best of our knowledge, this work is the first report of the direct observation of the reversible and continuous internal rotation of ferrocene in interlocked complexes in the single-crystal state using single-crystal X-ray crystallography. These behaviors are quite different from previously reported pseudorotaxanes with DB24C8.[26–30] We expect such unique interlocked complexes to strongly influence fundamental and application studies on organometallic complexes and molecular machines and switches. These interlocked complexes operating in the solid state would be useful in molecular building blocks, molecular ball-bearings, molecular toys, and molecular manipulations, storage of toxic solvents and would enable the tuning of mechanical properties of crystals. In addition, changing the molecular components (*e.g.*, by utilizing other metal centers, ammonium ions, or crown ethers) would bring about further unique molecular motions in crystals.

Author contributions

C.-H. W. carried out all experiments and wrote the first manuscript. K.-J. C., T.-H. W., and H.-K. C. synthesized compounds and carried out X-ray measurements. Y. T., Y. S., and P.-L. C.

supported the X-ray measurements. M. H. inspired the ideas, organized the whole project, and wrote and edited the manuscript.

Conflicts of interest

There are no conflicts to declare.

Acknowledgements

We are grateful to Prof. K. Osakada of Tokyo Institute of Technology for enlightening discussion. This work was financially supported by Ministry of Science and Technology Taiwan and National Tsing Hua University.

References

1 A. Togni and T. Hayashi, *Ferrocenes: homogeneous catalysis, organic synthesis, materials science*, VCH, Weinheim, 1995.
2 P. Stepnicka, *Ferrocenes: ligands, materials and biomolecules*, John Wiley & Sons, Chichester, 2008.
3 S. Ø. Scottwell and J. D. Crowley, *Chem. Commun.*, 2016, **52**, 2451–2464.
4 D. Astruc, *Eur. J. Inorg. Chem.*, 2017, 6–29.
5 J. Wei and P. L. Diaconescu, *Acc. Chem. Res.*, 2019, **52**, 415–424.
6 A. Straube, P. Coburger, L. Dütsch and E. Hey-Hawkins, *Chem. Sci.*, 2020, **11**, 10657–10668.
7 R. A. Musgrave and I. Manners, *Nat. Chem.*, 2016, **8**, 819–820.
8 J. Berger, M. Ondráček, O. Stetsovych, P. Malý, P. Holý, J. Rybáček, M. Švec, I. G. Stará, T. Mančal, I. Starý and P. Jelínek, *Nat. Commun.*, 2020, **11**, 1337.
9 R. L. N. Hailes, A. M. Oliver, J. Gwyther, G. R. Whittell and I. Manners, *Chem. Soc. Rev.*, 2016, **45**, 5358–5407.
10 W.-Y. Sun, T. Kusukawa and M. Fujita, *J. Am. Chem. Soc.*, 2002, **124**, 11570–11571.
11 G. Brunet, D. A. Safin, K. Robeyns, G. A. Facey, I. Korobkov, Y. Filinchuk and M. Murugesu, *Chem. Commun.*, 2017, **53**, 5645–5648.
12 N. Mohammadi, A. Ganesan, C. T. Chantler and F. Wang, *J. Organomet. Chem.*, 2012, **713**, 51–59.
13 C. P. Brock and Y. Fu, *Acta Crystallogr., Sect. B: Struct. Sci.*, 1997, **53**, 928–938.
14 D. Paliwoda, K. Kowalska, M. Hanfland and A. Katrusiak, *J. Phys. Chem. Lett.*, 2013, **4**, 4032–4037.
15 J. C. Bear, J. K. Cockcroft and J. H. Williams, *J. Am. Chem. Soc.*, 2020, **142**, 1731–1734.
16 M. T. Islam, S. P. Best, J. D. Bourke, L. J. Tantau, C. Q. Tran, F. Wang and C. T. Chantler, *J. Phys. Chem. C*, 2016, **120**, 9399–9418.
17 A. Haaland and J. Nilsson, *Acta Chem. Scand.*, 1968, **22**, 2653–2670.
18 A. M. Orendt, J. C. Facelli, Y. J. Jiang and D. M. Grant, *J. Phys. Chem. A*, 1998, **102**, 7692–7697.
19 X. Xia, H. Yu, L. Wang and Z. ul-Abdin, *RSC Adv.*, 2016, **6**, 105296–105316.
20 M. Malischewski, M. Adelhardt, J. Sutter, K. Meyer and K. Seppelt, *Science*, 2016, **353**, 678.
21 J. F. Stoddart, *Angew. Chem., Int. Ed.*, 2017, **56**, 11094–11125.
22 B. L. Feringa, *Angew. Chem., Int. Ed.*, 2017, **56**, 11060–11078.
23 J. P. Sauvage, *Angew. Chem., Int. Ed.*, 2017, **56**, 11080–11093.
24 S. Erbas-Cakmak, D. A. Leigh, C. T. McTernan and A. L. Nussbaumer, *Chem. Rev.*, 2015, **115**, 10081–10206.
25 D. Dattler, G. Fuks, J. Heiser, E. Moulin, A. Perrot, X. Yao and N. Giuseppone, *Chem. Rev.*, 2020, **120**, 310–433.
26 M. Horie and C.-H. Wang, *Mater. Chem. Front.*, 2019, **3**, 2258–2269.
27 M. Horie, Y. Suzaki, D. Hashizume, T. Abe, T. Wu, T. Sassa, T. Hosokai and K. Osakada, *J. Am. Chem. Soc.*, 2012, **134**, 17932–17944.
28 K.-J. Chen, Y.-C. Tsai, Y. Suzaki, K. Osakada, A. Miura and M. Horie, *Nat. Commun.*, 2016, **7**, 13321.
29 S.-C. Cheng, K.-J. Chen, Y. Suzaki, Y. Tsuchido, T.-S. Kuo, K. Osakada and M. Horie, *J. Am. Chem. Soc.*, 2018, **140**, 90–93.
30 S.-C. Cheng, C.-H. Wang, Y.-C. Lin, Y. Tsuchido, Y. Suzaki, Y. Sei, T.-S. Kuo and M. Horie, *ACS Appl. Mater. Interfaces*, 2020, **12**, 50002–50010.